Mathematical model and computer simulations of telomere loss

Ana Martinčić Špoljarić [a,1,*], Ivica Rubelj[b], Miljenko Huzak[c]

[a] *Faculty of Civil Engineering, University of Zagreb, Fra Andrije Kačića Miošića 26, 10000 Zagreb, Croatia*
[b] *Ruđer Bošković Institute, Bijenička 54, 10000 Zagreb, Croatia, Email: irubelj@irb.hr*
[c] *Department of Mathematics, Faculty of Science, University of Zagreb, Bijenička 30, 10000 Zagreb, Croatia, E-mail : miljenko.huzak@math.hr*

Abstract

Molecular mechanisms that control the limited number of human cell divisions have occupied researchers ever since its first description in 1961. There is evidence that this limited growth capacity, referred to as cellular or replicative senescence, is the basis for organismal aging. Numerous studies point to molecular mechanisms of telomere involvement in this phenomenon. Hallmark of cell senescence is high stochasticity where individual cells enter senescence in completely random and stochastic fashion. Therefore, a mathematical modelling and computational simulations of telomere dynamics are often used to explain this stochastic nature of cell aging. Models published thus far were based on the molecular mechanisms of telomere biology and how they dictate the dynamics of cell culture proliferation. In present work we propose advanced model of telomere controlled cell senescence based on the abrupt telomere shortening, thus explaining some important, but so far overlooked aspects of cell senescence. We test our theory by simulating the proliferative potential and two sister experiment originally conducted by Smith and Whitney in 1980.

Keywords: replicative senescence, abrupt shortening, human fibroblasts, stochastic cell aging dynamics, incomplete replication

*Corresponding author:
Email address: amartincic@grad.hr (Ana Martinčić Špoljarić)
URL: www.grad.unizg.hr/ana.martincic (Ana Martinčić Špoljarić)
[1] Declarations of interest: none

1. Introduction

The concept of cellular immortality in culture vs. organism was definitively rejected in 1961. thanks to the work of Paul Moorhead and Leonard Hayflick [1] who demonstrated that human fibroblasts cease dividing after approximately $50-60$ divisions when they permanently enter G1 phase of the cell cycle. Cells that reached their dividing limit, called Hayflick limit, undergo characteristic morphological and biochemical changes known as replicative senescence, also commonly perceived as ageing at the cellular level. Hayflicks experiments in late '60s and early '70s demonstrated a big variation of in vitro lifespan among cell cultures [2] and among lifespans of individual clones selected from the same cell culture [3].

Heterogeneity in proliferative potential of single clone of normal human fibroblast was best described by Smith and Whitney in 1980 [4]. In this experiment a single clone was isolated from a mass culture of human embryonic lung fibroblasts at population doublings (PD) 23. During the population growth of this clone, $100-200$ subclones were isolated at PD 39, 49 and 59 and proliferative potential was determined for each of them. At all sample points heterogeneity in remaining proliferative potential appeared to be stochastic, resulting in a distinct bimodal distribution of their PD potentials (Figure 1).

Additionally, Smith and Whitney conducted a "two-sister experiment" in which they proved that the degree of difference in doubling potential between two sister cells (cells arising from a single mitosis) may vary anywhere between 0 and 8 PDs (Figure 2).

In 1973 Olovnikov [5] suggested that DNA replication complex can not fully replicate both strands of chromosome ends known as telomeres. He proposed Theory of Marginotomy which predicts that such continuous shortening of telomeres with each cell division will result in limited cell proliferation. Later, it has been confirmed that telomeres indeed gradually shorten on average about 75 to 200 nucleotides with each round of division in normal human cells [6].

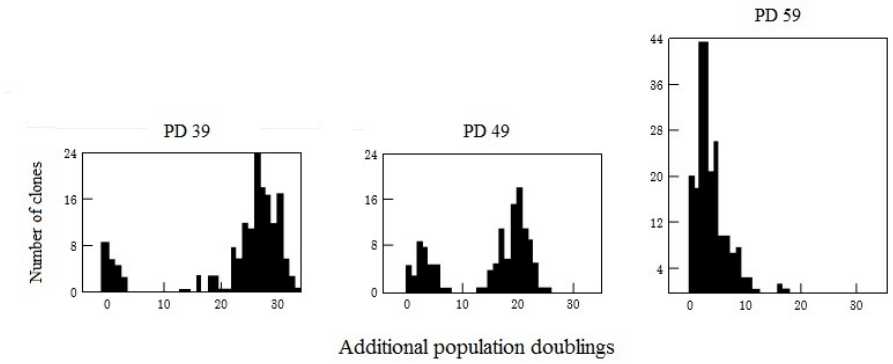

Figure 1: Smith-Whitney experiment that showed bimodal distribution in proliferative potential of normal human fibroblasts. From a monoculture that underwent 23 PDs an individual cell was selected and left to divide. At PD 39, 49 and 59, between 100 and 200 subclones were isolated and their proliferative capacity was determined. (Adapted from Smith and Whitney, 1980 [4])

Soon it became clear that results obtained by Smith and Whitney couldn't be explained only by this gradual telomere shortening. In order to account for this phenomenon, different explanations for the sudden appearance of senescent cells in culture have been suggested. Among others, Elizabeth Blackburn suggested a stochastic model of telomere uncapping [7], von Zglinicki studied accelerated shortening of telomeres in the sub-population of cells [8] and Rubelj and Vondraček proposed theoretical model of abrupt telomere shortening [9]. The latest model implies sudden and stochastic telomere shortening and the emergence of extra-chromosomal circular telomeric DNA molecules (the t-circles) as a result of recombinational resolution of Holliday's structure at the border of the subtelomeric and telomeric region. Presence of t-circles has been shown in different cell cultures, such as yeast cells [10, 11], in some tumor cell lines [11, 12, 13, 14, 15, 16] and especially in cells that maintain their telomeres by recombination ALT mechanism [17]. In the year 2010 presence of t-circles has been confirmed in normal human skin and lung fibroblasts, MJ90 and IMR90 [18]. Abrupt telomere shortening provide plausible explanation for quick gener-

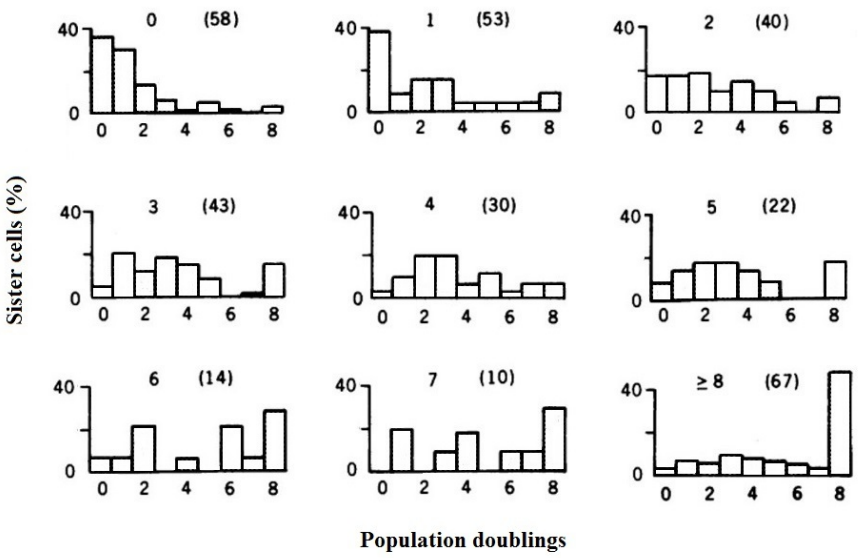

Figure 2: Smith-Whitney two-sister experiment that demonstrated variation in proliferative potential between cells arising from single mitotic events. Histograms represent number of population doublings of cells whose sister cells were able to undergo the indicated number of doublings. All cells that underwent more than 8 PDs (≥ 256 cells) are considered as a single category. Number of analysed sister cells are given in parentheses. (Adapted from Smith and Whitney, 1980 [4])

ation of heterogeneity in PD potential among clonal cell culture, but still some important issues must be addressed. In current model, if one telomere lose large portion of its sequence due to deletion, all cells from its branching fraction carrying such short telomere will have less remaining PDs because the shortest telomere in the cell will first lose its stable structure and be recognized as DNA damage causing cell cycle arrest in G1. Since human telomeres are repetitive sequences, theoretically such abrupt shortening could result in deletions of various lengths. That would result in subclones with PDs spread anywhere between maximal to minimal dividing potential and not in strict bimodal distribution observed by Smith and Whitney. In order to provide better explanation for this phenomenon, in this paper we present improved molecular model and its mathematical simulations with some crucial features without which cell senescence

can not be fully understood.

2. Results

2.1. Biological model of the loss of telomere sequences of a chromosome

Chromosomes are thread-like structures of DNA and proteins that get replicated and passed on from parents to offspring. Humans have 23 pairs of chromosomes in their cells, of which 22 pairs are autosomes and one pair of sex chromosomes, making a total of 46 chromosomes in each cell. Telomeres are repetitive sequences at chromosome's ends and they play crucial role in protection of chromosome integrity and genome stability. Human telomeres, like in all vertebrates consist of repetitive TTAGGG sequences, with the complementary DNA strand being AATCCC. Telomeres are dynamic structures in the way that in normal somatic cells they shorten with each division. When at least one telomere is critically short, it lose its protective function, which leads to permanent cell replication arrest. Therefore, telomeres are directly responsible for chromosome stability, cell ageing and senescence.

DNA consists of two complementary antiparallel $5' \rightarrow 3'$ and $3' \rightarrow 5'$ strands. During replication, the double-stranded DNA gets separated and each parent strand serves as a template for synthesis of its counterpart. DNA replication begins at specific points on the chromosome called origins of replication. Unzipping of DNA at the origin results in formation of two replication forks (Figure 3) growing bi-directionally from the origin. Replication starts with synthesis of short RNA primer on single stranded DNA (ssDNA) by enzyme DNA primase. RNA primers serves as initiating points for synthesis of DNA by DNA polymerase. Polymerase works only in one direction, thus replication starts at the $5'$ end of both new strands and moves in the $5'$ to $3'$ direction. The new strand which is continuously synthesized in the same direction as the growing replication fork is called *leading* strand, while the other strand that is synthesized discontinuously in short $5'$ to $3'$ segments called Okazaki fragments is *lagging* strand [19].

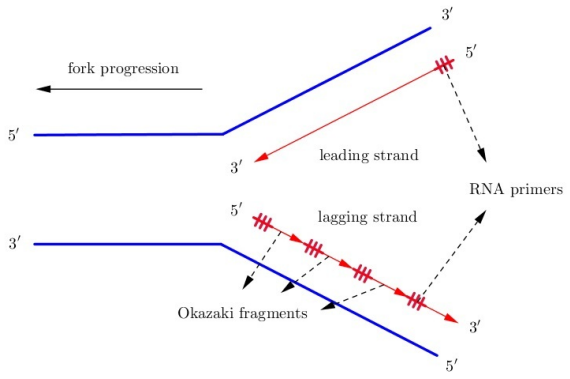

Figure 3: During the first step of DNA replication DNA helicase untwists the helix at replication origins in order to separate two DNA strands. The replication origin forms a replication bubble, consisted of two Y shaped replication forks (because of symmetry, here we show only one). The thicker blue lines represent the template (parent) strands, while the thinner red lines represent the newly replicated strands and the arrows show the direction of replication ($5'$ to $3'$ on the new strands).

After the removal of RNA primers, gaps between Okazaki fragments are filled by DNA polymerase and connected by DNA ligase creating continuous double stranded DNA. The processing of the last RNA primer leaves the $5'$ end of the new strand shortened, thus creating the single stranded $3'$ overhang of the parental telomere. On the other end of the chromosome leading strand will create blunt end. The process is known as the end-replication problem and was first suggested by Olovnikov in the early 1970s [20, 5]. New findings revel that $5'$ - exonucleolitic degradation of C-rich chain regenerates a $3'$ end overhang structure on both telomeres at chromosome ends [21, 22, 23]. Although the number of telomere repeats loss varies among chromosome ends, experimental data shows that average telomere loss between $50-200$ basepairs per replication [24], starting in the range $\approx 7000-25000$ for human fibroblasts.

Most previous mathematical models of telomere shortening assumed that telomere loss occurs only as a result of incomplete replication of the lagging strand [25, 22, 26, 27], but lately models have been suggested that took in the

consideration the additional processing of the parent strand [21, 22, 23]. We build on that theory and present a model that considers and explains abrupt shortening in more detail.

Since abrupt telomere deletion has been confirmed in dividing cultures resulting in strict bimodal distribution of their subclones, it appear obvious that deletions have some restrictions on where along telomere lengths they can occur. Rational for this is the following, since telomeres are repetitive sequences, single stranded 3' end could (self)invade at any position along telomere repeats. This would result in subclones with PD potentials that are not strictly bimodal but spread anywhere between maximal and minimal PDs. Therefore, we propose that there is a "hotspot" or narrow region near telomere/subtelomere border sequence prone to self-recombinational deletion. In this way full length telomere, regardless of its current length achieved by gradual shortening, would engage self-recombination exclusively close to its border region. Therefore, middle part of telomere repeats would be skipped in these recombinational events generating subpopulation of cells with fewer, 0 to 8 PDs. Here we provide mathematical model that explains such sequence of events.

Beside end-replication and additional parent strand processing, it is known that there are other mechanisms and factors that also contribute to telomere shortening, like environmental stress [28], single strand breaks [29] and oxidative stress [8, 22]. However, since the prime goal of this article is simulation of Smith and Whitney's experiments, which had been conducted *in vitro* in controlled environment, our focus will remain on the problems described at the beginning of this chapter.

2.2. Mathematical model of the loss of telomere sequences of a chromosome

The mathematical model that we propose describes shortening of telomeres by both incomplete replication and abrupt shortening, taking into account new findings about maturation steps on the leading strand. Shortening due to the end-replication problem and $5'$ - exonucleolitic degradation of C-rich chain will be considered regular (or gradual) shortening and the idea of abrupt shortening

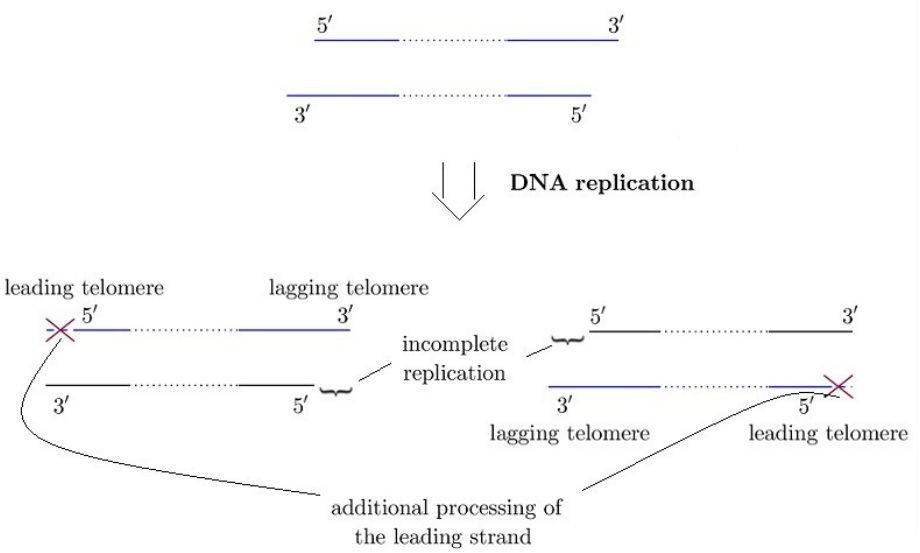

Figure 4: Through DNA replication each chromosome generates two new chromosomes of different telomere lengths.

is based on the model developed by Rubelj and Vondraček in 1999 ([9]). While in [9] authors considered deterministic gradual shortening in which chromosomes always produce two daughters, one of the same telomere length and one shortened for exactly one deletion unit, our model is completely stochastic and takes into consideration new knowledge about shortening of the parent strand. Furthermore, we introduce probability of abrupt shortening given specific telomere length partially based on experimental data.

Models based only on regular telomere shortening have been considered before, both deterministic [25, 26] and stochastic [30, 31, 22, 32, 21, 33, 34, 35, 36]. However, unlike in model we present here, stochastic gradual shortening was usually simplified, except in models of pure theoretical interest (e.g. [27]). We present telomere loss in terms of what happens to single DNA strands in S phase of the cell cycle (following description by Levy and co-workers [26]). During the G_1 phase, before DNA replication, chromosomes are composed of only one chromatid consisting of two antiparallel DNA strands designated as *upper*

(or $5' \to 3'$) and *lower* (or $3' \to 5'$). Each strand has two ends named *left* and *right*. For each of the $k = 1, \ldots, 46$ chromosomes, numbers of telomeric deletion units (number of nucleotides in telomeric region) in the nth generation on both ends of both strands are represented by a 2×2 matrix

$$\begin{pmatrix} X_n^k & Y_n^k \\ Z_n^k & W_n^k \end{pmatrix}. \tag{1}$$

The first row represents left and right end of the upper strand, while the second row represents left and right end of the lower strand. During division each of the 46 chromosomes divides into two new daughter chromosomes following rules described below. Chromosomes biologically behave independently one of another, so mathematically we can observe this divisions as 46 independent processes. Therefore, we will study the behaviour of only one chromosome and for the simplicity of notation omit index k from the representation matrix:

$$\begin{pmatrix} X_n & Y_n \\ Z_n & W_n \end{pmatrix}. \tag{2}$$

For the simplicity of the model and simulation we assume that the initial newborn cell consists of the same number of deletion units on both ends of both strands of each of the 46 chromosomes. Naming the initial number (in the 0th generation) of deletion units with N, representation of the new chromosome will thus be

$$\begin{pmatrix} X_0 & Y_0 \\ Z_0 & W_0 \end{pmatrix} = \begin{pmatrix} N & N \\ N & N \end{pmatrix}. \tag{3}$$

First, we present the model without abrupt telomere shortening. During replication telomeres on the leading and lagging strand of a chromosome shorten as described in Section 2.1. Both $5'$ ends of both new chromosomes are shortened for random number of nucleotides with respect to a parent chromosome. Based on available experimental data (e.g. [8, 37]) we may assume that telomeres shorten according to uniform random variables C_n^i, D_n^i, $i = 1, 2$. Variable D_n^i represents telomere loss (in bases) due to shortening on the newly synthesized

chain of the ith chromosome daughter in the nth generation, while variable C_n^i represents telomere loss due to shortening on the parent chain of the ith chromosome daughter in the nth generation, due to maturation steps mentioned before. Shortenings of the parent and newly synthesized chain are independent and approximately of the same rate, so we may assume that variables C_n^i and D_n^i, $i = 1, 2$ are independent and identically distributed discrete random variables uniformly distributed over interval (a, b). As mentioned in Section 2.1, experimental data shows that telomeres lose $50 - 200$ base pairs per replication, and we will use those numbers to be interval limits a and b.

Summing up the above rules, chromosome of the nth generation will produce two new chromosomes shorter for some random number of nucleotides on their $5'$ ends. This translates into the following transition rules for representation matrices (parent strands are printed in blue and newly synthesized strands in black):

$$\begin{pmatrix} X_n & Y_n \\ Z_n & W_n \end{pmatrix} \to \begin{cases} \begin{pmatrix} X_n - C_n^1 & Y_n \\ X_n & Y_n - D_n^1 \end{pmatrix} \\ \\ \begin{pmatrix} Z_n - D_n^2 & W_n \\ Z_n & W_n - C_n^2 \end{pmatrix}. \end{cases} \tag{4}$$

The whole process can be seen on Figure 5a.

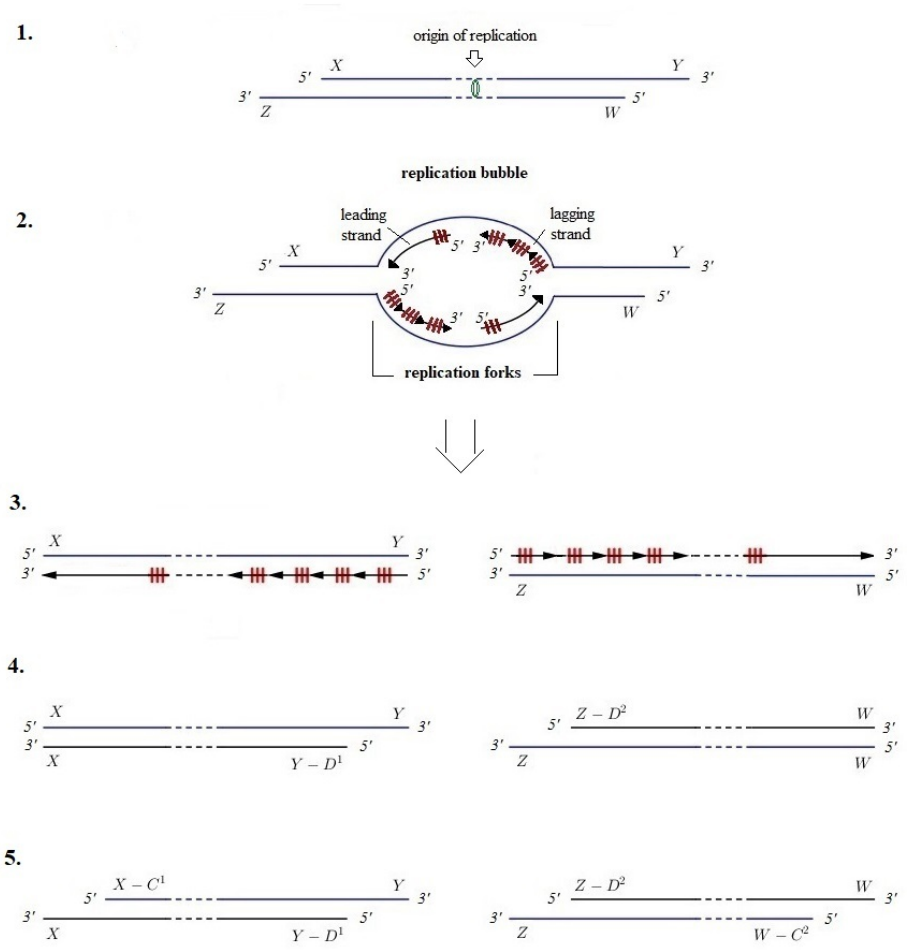

(a) Both daughters underwent regular shortening, i.e. $B^1 = 0$ and $B^2 = 0$ **1.** Parent chromosome with telomere lengths X, Y, Z, W, disregarding cell generation for simplicity **2.** Replication starts at points of origin. After forming replication bubbles, DNA polymerase synthesizes new strands in $5' \to 3'$ direction. **3.** The "untangled" version of the previous step where two new chromosomes are separated. **4.** After the removal of RNA primers, Okazaki fragments are joined together by DNA ligase. Last Okazaki fragments on the $5'$ ends of newly synthesized strands leave those ends shortened for some random number of nucleotides D^1 and D^2 **5.** Additional telomere shortening on the parent strand leaves $5'$ ends of parent strands shorter for random number of nucleotides C^1, i.e. C^2.

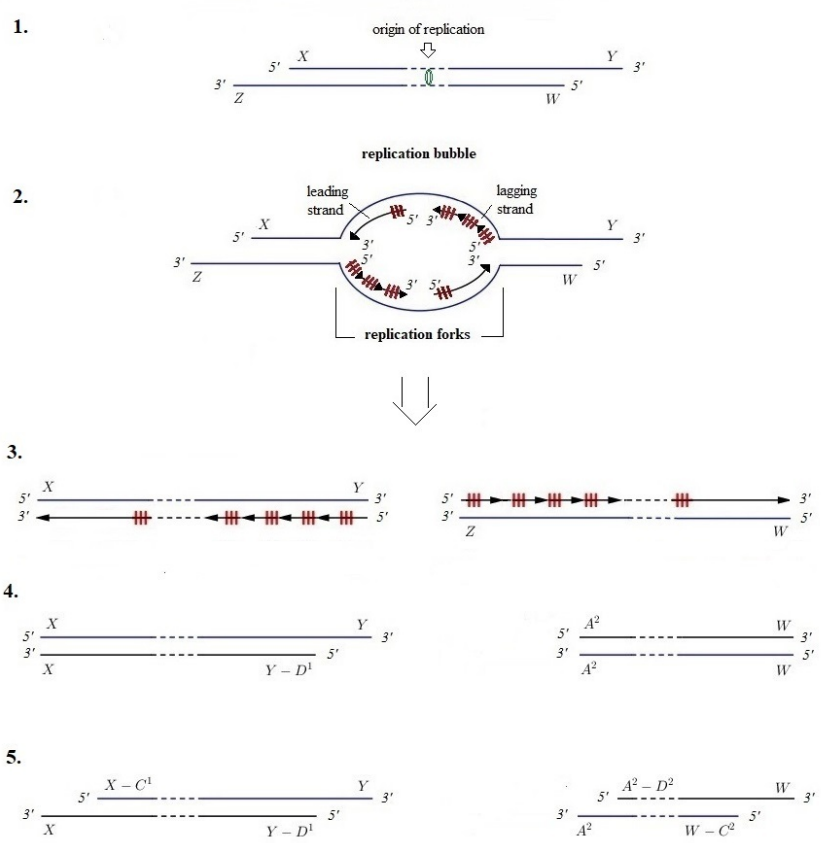

(b) First daughter underwent regular shortening and second daughter underwent abrupt shortening, i.e. $B^1 = 0$ and $B^2 = 1$. First three steps remain the same as in 5a. During the step number 4. when t-loop is formed, in case of invasion of single-strand $3'$ end in improper site close to border region designated as hotspot a recombination will occur resulting in telomere repeat deletion. Fifth step again stays the same because additional telomere shortening on the $5'$ end of the parent strand happens on both new daughter chromosomes.

Figure 5: Steps of telomere shortening during chromosome replication

However, we claim that this is not the only shortening mode and we introduce abrupt shortening, following [9]. Abrupt shortening can only occur on the $5'$ end of newly synthesized chain and it shortens both upper and lower strand of the affected end. Probability that a chain will undergo abrupt shortening depends on it's length (number of remaining telomeric nucleotides), see Appendix A, and is here modelled through the Bernoulli random variables B_n^i, $i = 1, 2$, "success" being the occurrence of an abrupt shortening. If an abrupt shortening happens (if $B_n^i = 1$), affected strand (and its parent strand) will shorten to the length A_n^i, where every A_n^i is a discrete random variable uniformly distributed over interval (c_1, c_2), i.e. $A_n^i \sim U(c_1, c_2)$, $i = 1, 2$. Thus, length of the both upper and lower affected strand will fall into hotspot region (c_1, c_2), see Figure 5b. We assume that the chain can undergo abrupt shortening only if the length of the chain exceeds the upper hotspot limit c_2. Moreover, $5'$ end that had been shorten will undergo one more regular shortening, thus reconstructing the $3'$ overhang. Additional regular shortening of the $5'$ end will again be modelled by uniformly distributed random variables D_n^i, $i = 1, 2$ over interval (a, b).

Summarizing all of the above, we get following transition rules for representing matrices:

$$\begin{pmatrix} X_n & Y_n \\ Z_n & W_n \end{pmatrix} \to \begin{cases} \begin{pmatrix} X_n - C_n^1 & B_n^1 A_n^1 + (1 - B_n^1) Y_n \\ X_n & B_n^1 A_n^1 + (1 - B_n^1) Y_n - D_n^1 \end{pmatrix} \\ \\ \begin{pmatrix} B_n^2 A_n^2 + (1 - B_n^2) Z_n - D_n^2 & W_n \\ B_n^2 A_n^2 + (1 - B_n^2) Z_n & W_n - C_n^2 \end{pmatrix} \end{cases} \tag{5}$$

The process ends when one of the telomere ends becomes short enough. Without loss of generality, we assume that it happens when all telomeric nucleotides (on either end of either strand) are lost, i.e. when a zero appears in the representing matrix, which will typically occur on one of the $5'$ ends, see

(6).

$$\begin{pmatrix} 0 & Y_n \\ Z_n & W_n \end{pmatrix}, \quad \begin{pmatrix} X_n & Y_n \\ Z_n & 0 \end{pmatrix}. \tag{6}$$

We can define the state of the chromosome in the nth generation to be the shortest of it's ends:

$$K_n = \min(X_n, Y_n, Z_n, W_n) = \min(X_n, W_n), \tag{7}$$

in which case the above process ends when K_n reaches zero. Considering the real biological setting, this assumption may not be realistic - but the same mathematics would apply in the case of telomere loss until a particular checkpoint is met.

After replication, chromosomes get randomly separated into two new cells. When a cell gets a chromosome that stopped dividing (reached zero anywhere in the representation matrix), we shall consider it senescent. Since the shortest chromosome determines the end of replicative lifespan of a cell, we can denote the state of a cell in the nth generation as

$$L_n = \min_{k=1,\ldots,46} K_n^k. \tag{8}$$

The assumption is biologically reasonable because all senescent cells remain viable and accumulate until ultimately whole culture is senescent [1, 2]. In our model (and simulation) senescent cells have a single progeny of the same type as the parent cell, i.e. they reproduce themselves.

3. Simulation algorithms

Based on the mathematical model from the Section 2.2 we tried to simulate the experiments (hereinafter referred to as the "original" experiments) done by Smith and Whitney in the 1980 [4].

3.1. Model assumptions

Simulation algorithms presented in this section are based on the following assumptions and rules:

- Each cell consists of 46 chromosomes which are represented with matrix (2) and follow transition rules (5).

- Telomere elongation due to telomerase activity or any other reason has not been considered.

- A cell that becomes senescent will remain in that state (it cannot start dividing again) and continue to exist in the population. Since we simulate experimental results obtained with cell culture, we do not consider apoptosis (cell death).

- Abrupt shortening can occur only on newly synthesized chain.

- Abrupt shortening cannot happen if telomere length reaches the upper limit of hotspot region c_2, i.e. if the parent chain becomes too short.

- Since our model implies synchronous divisions of all cells, which is not the case in the real biological setting, we decided to address the problem the same way as Rubelj and Vondraček in [9]. We assume that there is a probability of non-division for every cell in each cycle, which depends on telomere length (and indirectly the age of the cell). Cells with shorter telomeres (typically older cells) have a greater probability of skipping division in particular cycle:

$$\mathbb{P}(\text{cell non-division in the } n\text{-th generation}) = \alpha(1 - \frac{L_n}{N})^{\beta}, \qquad (9)$$

where $\alpha = 0.8$, $\beta = 4$ and L_n stands for telomeric state of the cell in the nth generation defined by (8).

All the simulations were carried out in *RStudio (Version 1.0.136)*.

3.2. Simulation algorithm of proliferative potential experiment

1. In the original experiment, one cell was randomly chosen from monoculture that underwent 23 population doublings. We started with a cell in

which all telomere endinggs (on each of the 46 chromosomes) had the initial values as shown in (3) with $N = 5500$ base pairs. We let her divide until the population size reached 24 population doublings and then randomly selected one cell. The resulting cell will be called the *mother cell*. Due to computer restrictions, we resampled the culture by keeping only 2^9 cells every time it's size surpassed 2^{10} cells.

2. The mother cell was then left to replicate until the population reached additional 16 population doublings. Taking into account first 23 divisions of the mother cell, we can assume that the obtained cells underwent 39 population doublings in total. Again, due to computer restrictions, we resampled the culture by randomly choosing 2^9 cells every time the population size exceeded 2^{10}. When the population size reached targeted population doublings, we randomly selected 200 cells. In the original experiment resampling was done when the cells became confluent. Cells were then trypsinized and split in 1:4 ratio and seeded into new flasks, thus each split occured after 2 PDs.

3. For each of 200 selected cells we needed to determine their population doubling potential. Considering that it would be time and memory extremely consuming, at this step only the chromosome with the shortest telomere was left to represent the cell. It has been shown that the initial shortest telomere plays the major role in controlling senescence, especially if there is a high variance of telomere length in a particular cell [33, 38, 21]. Even though we started with a cell that consisted of 46 identical chromosomes, at this point of culture growth there exists a significant heterogeneity among telomere lengths. Therefore, we presume that following only the shortest chromosome will provide us reasonable approximation of proliferative potential. We let the cell replicate until all cells in the population reached their terminal phase (at least one of the telomeres of the chromosome we kept following reached zero). If there were more then 2^{10} cells in the population, we randomly chose 2^8 and let them continue with divisions. When population consisted of only non-dividing cells, we counted

the cells and determined their PD (taking resampling into account).

4. After excluding 200 cells we chose in step number 2, we let the initial culture produce another 10 population doublings (summing up to 49 PDs considering 39 that the mother cell already underwent). We select 200 cells and calculate their population doubling potential as in previous step.
5. We exclude 200 cells selected in previous step and allow the mother cell to reach 59 PDs. Again, we select another 200 cells and calculate their population doubling potential as in step number 3.

Simulation results are shown in Figure 6. Since the age of the mother cell from the original experiment was unknown to us, initial telomere length N was chosen to fairly fit the experiment results from Figure 1. From the simulation results we can see there is a small "shift" in additional population doublings on each of the graphs, i.e. N should be somewhat smaller. However, our main idea was not to completely replicate the results but to show characteristic bimodal distribution in cell's proliferative potential, which can be clearly seen in Figure 6.

3.3. Simulation algorithm for two sister experiment

In the article published by Smith and Whitney [4] two sister experiment was not described in such detail as the experiment about proliferative potential. Therefore, we can only assume the exact procedure and try to reproduce the main idea of the experiment.

1. Again, we start with a cell in which all the chromosomes have the initial values as shown in (3). We let the cell achieve 50 population doublings and then randomly select 336 cells (number of analysed mitotic pairs in the original experiment). Resampling was done (by randomly choosing 2^9 cells) every time the population size exceeded 2^{10}.
2. Cells that we chose in the previous step will divide one more time. We keep both of their daughter cells and numerate them as Sister 1 and Sister 2.

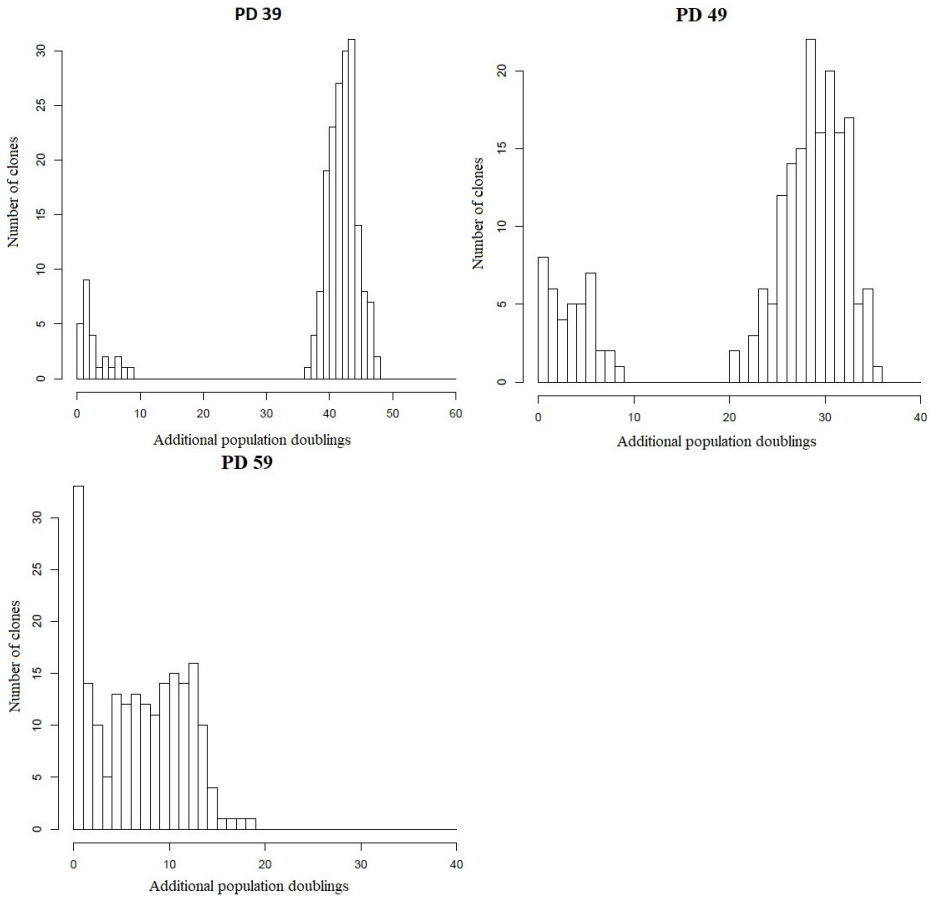

Figure 6: Computer simulation of the Smith and Whitney proliferative potential experiment. The exact parameters used: $N = 5500$, $a_1 = 50$, $b_1 = 200$, $\alpha = 0.8$, $\beta = 4$, $c_1 = 100$, $c_2 = 300$.

3. In order to determine population doubling potential of each daughter cell, we let them divide until they reach their replicative senescence. Again, in this step only the chromosome with the shortest telomere was left to represent the cell. Resampling was done as before.

4. We calculated population doublings of Sisters 1 and 2, taking resampling into consideration, and sorted the data by Sister 1. In original experiment all cells that produced more than 256 progeny were considered as a single category, but we had no such restrictions and counted the exact number of progeny of every sister.

290 Simulation results are shown in Figure 7. As before, due to lack of information about the original experiment we can not completely replicate the results in Figure 2. Instead, one should keep in mind that the idea was to show that proliferative potential of sister cells coming from the same mitotic event can differ greatly.

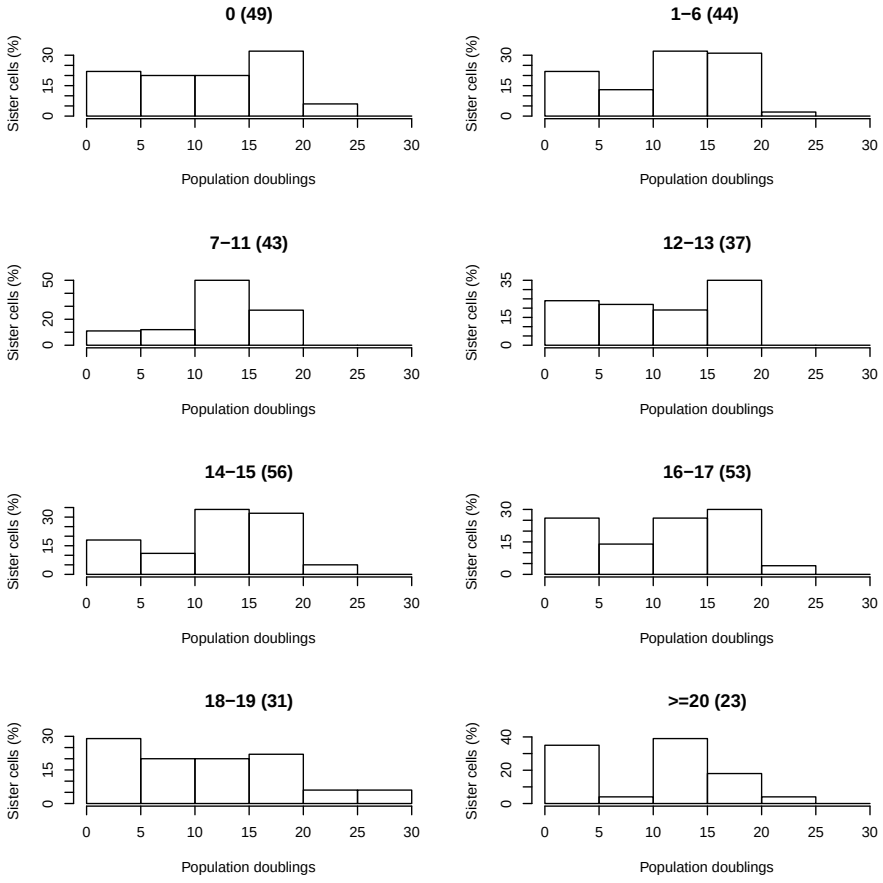

Figure 7: Computer simulation of the Smith Whitney two sister experiment. The exact parameters used: $N = 5500$, $a = 50$, $b = 200$, $\alpha = 0.8$, $\beta = 4$, $c_1 = 100$, $c_2 = 300$.

4. Discussion

In summary, we present a model that unites previous knowledge of regular and abrupt telomere shortening, extended by the new biological theory and mathematical model of the region that is hotspot for recombination. Because of complexity biological background of the hotspot theory is left to be explained in detail in an additional work. Shortly, transition from high PD potential to low PD potential among subclones, with no clones in between (strict bimodal distribution) indicates existance of hotspot for (self)recombination/deletion located near telomere/subtelomere border region. If this would not be the case and (self)recombination/deletion occurred anywhere along the telomere, clones with reduced dividing potential would scatter between maximal and minimal dividing potential and bimodal distribution would not be observed. Explanation for accelerated increase in frequency of (self)recombination/deletion on telomeres with increasing PDs observed in [8], comes from assumption that shorter telomeres have less time to finish lagging strand processing as replication fork proceedes. Unfinished processing of newly synthesized lagging strand may give DNA repair mechanisms oportunity to involve telomere 3' single strand end into recombination that can resolve in terminal deletion of telomere repeats [39]. So, the shorter the telomere, the higher the probability for (self)recombination/deletion. This model further implies that in described telomere repeat deletion primarely (or exclusively) lagging strand is involved.

Here, our focus remains on simulations of the well known Smith and Whitney experiment from the 1980. For the first time we carried out simulations of culture aging with all three modes of telomere shortening (incomplete end-replication, C-strand processing, abrupt telomere shortening) keeping the shortening rate random. Also, for the first time we simulated two sister experiment and showed diversity in proliferative potential of two sisters coming from the same mitotic event.

There are still some problems that are left to be addressed in the future. One of the drawbacks of current model is the assumption of simultaneous divisions

that we tried to compensate by including the probability of cell non-division in every cycle. Future theoretical mathematical model should consider incorporating cell lifetime distributions and other factors that influence cell division dynamics (such as contact inhibition). Many models have been developed for in vivo cell division, but that was beyond the scope of this article. In current model there is the absence of cell death or apoptosis, but this is biologically justified because Smith and Whitney experiments were performed with normal human fibroblasts in culture where no spontaneous apoptosis is observed. Although apoptosis does not play a major role in in vitro experiments, if one would like to explain real in vivo aging process, apoptosis must be considered.

During our simulations we kept track of the length of both strands of each telomere as long as it was possible. In order to simplify and accelerate our simulations in the last phase of every algorithm we decided to follow only the chromosome with the shortest telomere. Although difference in the results may be minimum, ideally we should consider an algorithm without such simplification.

Main goal for the future would be further development of theoretical model underlying our simulations and finding estimations of model parameters based on the real data. In order to do so we need to focus on collecting data necessary for estimating probabilities of abrupt shortening given by (A.1), i.e. (A.2) and explained in Appendix A. Probability distribution of telomere length in different cell types has been studied many times before [40, 41, 42]. Although it has been shown that the methods used in collecting and analysing those experimental data are imprecise ([43]), we can anticipate the shape and behaviour of the distribution. However, both probability distributions of abrupt shortening and telomere length depend on generation n of the cell containing the particular chromosome, or, biologically more relevant, they depend on the cell population doubling. In order to assess those two probabilities, we should obtain experimental data on the growth of the same cell monoculture after different population doublings. Ideally, we should repeat Smith and Whitney's experiment with known parameters (such as the initial telomere length of the mother

cell, exact conditions of cell transferring etc.) and every time we stop to isolate 200 cells at some specific population doubling, we should also find distribution of telomere length of those cells.

Acknowledgements

This work has been fully supported by Croatian Science Foundation under the project 3526.

Appendix A. Modelling the probability of abrupt shortening

In this appendix we will describe how we model the probability of abrupt shortening as a function of the chain length by using the available data.

Let U_n be the length of the $3'$ end of parent strand in the nth generation immediately before the shortening, i.e. $U_n = Y_n$ or $U_n = Z_n$ (see Section 2.2). There are two "modes" of shortening that we consider:

$\mathcal{R} = \{B_n = 0\}$ - regular shortening,

$\mathcal{A} = \{B_n = 1\}$ - abrupt shortening.

Here, B_n denotes Bernoulli variables B_n^1 or B_n^2, indicators of abrupt shortening (see Section 2.2). Let us denote by $\mathbb{P}(\mathcal{A} \mid U_n = k)$ the probability that the chain of the length k and generation n undergoes the abrupt shortening. Through the Bayes' theorem we have:

$$\begin{aligned}
\mathbb{P}(\mathcal{A} \mid U_n = k) &= \frac{\mathbb{P}(U_n = k \mid \mathcal{A})\mathbb{P}(\mathcal{A})}{\mathbb{P}(U_n = k)} \\
&= \frac{\mathbb{P}(U_n = k \mid \mathcal{A})\mathbb{P}(\mathcal{A})}{\mathbb{P}(U_n = k \mid \mathcal{A})\mathbb{P}(\mathcal{A}) + \mathbb{P}(U_n = k \mid \mathcal{R})\mathbb{P}(\mathcal{R})} \\
&= \frac{\mathbb{P}(U_n = k \mid \mathcal{A})\mathbb{P}(\mathcal{A})}{\mathbb{P}(U_n = k \mid \mathcal{A})\mathbb{P}(\mathcal{A}) + \mathbb{P}(U_n = k \mid \mathcal{R})(1 - \mathbb{P}(\mathcal{A}))} \\
&= \frac{\mathbb{P}(U_n = k \mid \mathcal{A})\mathbb{P}(\mathcal{A})}{\mathbb{P}(\mathcal{A})(\mathbb{P}(U_n = k \mid \mathcal{A}) - \mathbb{P}(U_n = k \mid \mathcal{A})) + \mathbb{P}(U_n = k \mid \mathcal{R})} \\
&= \frac{\mathbb{P}(U_n = k \mid \mathcal{A})\mathbb{P}(\mathcal{A})}{\mathbb{P}(U_n = k \mid \mathcal{R})} \cdot \frac{1}{1 + \mathbb{P}(\mathcal{A})(\frac{\mathbb{P}(U_n = k \mid \mathcal{A})}{\mathbb{P}(U_n = k \mid \mathcal{R})} - 1)}.
\end{aligned} \tag{A.1}$$

As it was stated in [18] abrupt shortening is a rare event that can not affect more than a few percent of cells at any time. Otherwise cells wouldn't be able to reach their known proliferative potential (MJ90 cultures achieve more then 60 PDs, which means more then 100 cell generations). Therefore, $\mathbb{P}(\mathcal{A}) = p_n$ has been estimated in [18] to be very small ($\approx 5 \cdot 10^{-4}$) and we get

$$\mathbb{P}(\mathcal{A} \mid U_n = k) \approx \frac{\mathbb{P}(U_n = k \mid \mathcal{A})\mathbb{P}(\mathcal{A})}{\mathbb{P}(U_n = k \mid \mathcal{R})} \tag{A.2}$$

We now turn our focus to $\mathbb{P}(U_n = k \mid \mathcal{A})$. Denoting with V_n the part of the telomere that was lost in the nth generation abrupt shortening, we have

$$\begin{aligned}
\mathbb{P}(U_n = k \mid \mathcal{A}) &= \mathbb{P}(V_n + A_n = k) \\
&= \sum_{a=c_1}^{c_2} \mathbb{P}(V_n = k - a \mid A_n = a)\mathbb{P}(A_n = a) \\
&= \frac{1}{c_2 - c_1 + 1} \sum_{a=c_1}^{c_2} \mathbb{P}(V_n = k - a) \\
&\approx \mathbb{P}(V_n = k - \frac{c_1 + c_2}{2}).
\end{aligned}$$

Here, A_n denotes uniformly distributed variable A_n^1 or A_n^2 over hotspot range (c_1, c_2) (see Section 2.2). Above we also assume that V_n and A_n are independent random variables.

To estimate the above probability we can use data about extrachromosomal t-circles from [18]. Since we accept the theory that telomere circles come exclusively from abrupt shortening, their length coincides with the definition of variable V_n. Therefore relative frequencies of distribution of t-circle sizes from [18] can be used to obtain the law of V_n, i.e. probabilities $\mathbb{P}(V_n = k)$ for $k > 0$.

Although it would be a reasonable assumption that these data also depend on cell generation (and telomere length), studied cell culture wasn't monoculture and we cannot say anything specific about the age of cells taken into account. Therefore, we merged all collected data and, having in mind that the size of t-circles was measured in bases, we were looking for a best fit among discrete distributions that were biologically meaningful (such as Poisson distribution,

binomial distribution etc.) The negative binomial distribution describes the experimental data fairly accurately, see Figure A.8.

Since we already concluded that the other two probabilities (i.e. $\mathbb{P}(\mathcal{A})$ and $\mathbb{P}(U_n = k \mid \mathcal{R})$) cannot be estimated from available data, we assumed they depend only on telomere length k and we tried to find the function that would best reproduce results from Smith and Whitney proliferative potential experiment. Ratio of two aforementioned probabilities, $\mathbb{P}(\mathcal{A})/\mathbb{P}(U_n = k \mid \mathcal{R})$, is in our simulations modeled with logistic power function

$$h(k) \equiv h(k; a, b, c) = \frac{a}{1 + \left(\frac{k}{b}\right)^c},$$

where k stands for telomere length on the $3'$ end of the parent strand. Hence, we used for simulation

$$\mathbb{P}(\mathcal{A} \mid U_n = k) := h(k)\mathbb{P}(V = k - \frac{c_1 + c_2}{2}) \tag{A.3}$$

where V is equal to V_n in law and does not depend on cell generation n. Parameters a, b and c of function h are estimated by an iterative least-squares (LS) procedure from the cumulative relative frequencies of abrupt shortening up to an achieved population doublings calculated from Smith and Whitney data ([4]) in [9]. More precisely, let $\mathrm{CP}(PD)$ represent the expected cumulative relative frequency (or cumulative probability) of abrupt shortening up to an achieved population doublings. Then

$$\mathrm{CP}(PD) \approx \frac{1}{2^{PD}} \sum_{pd \leq PD} \mathbb{P}_{pd}(\mathcal{A}_{cell}) M(pd),$$

where $\mathbb{P}_{pd}(\mathcal{A}_{cell})$ represents the probability that at least one telomere sequence went through abrupt shortening if the culture has achieved pd population doublings, and $M(pd)$ is a number of cells in a culture achieving one cell generation less then full pd populationg doublings and which have not been abrupt shorten yet (none of the cells chromosomes underwent abrupt shortening). Since $p_n = \mathbb{P}(\mathcal{A})$ is a small number, it follows that

$$\mathbb{P}_{pd}(\mathcal{A}_{cell}) = 1 - (1 - p_n)^{46} \approx 46 p_n.$$

Let $N_{pd}(n)$ be a number of cells among that accounted in $M(pd)$ which have achieved n generations. Since

$$\mathbb{P}(\mathcal{A}) = \sum_k \mathbb{P}(\mathcal{A} \cap \{U_n = k\}) \overset{(A.2)}{\approx} \sum_k \mathbb{P}(\mathcal{A}|U_n = k)\mathbb{P}(U_n = k|\mathcal{R}) \overset{(A.3)}{=}$$
$$= \sum_k h(k)\mathbb{P}(V = k - \frac{c_1 + c_2}{2})\mathbb{P}(U_n = k|\mathcal{R})$$

by taking in account approximation (A.2) and definition (A.3) of $\mathbb{P}(\mathcal{A}|U_n = k)$, approximation of $\mathbb{P}_{pd}(\mathcal{A}_{cell})$ and $M(pd) = \sum_n N_{pd}(n)$ we get

$$\mathrm{CP}(PD) \approx \frac{46}{2^{PD}} \sum_{pd \le PD} \sum_n \sum_k h(k)\mathbb{P}(V = k - \frac{c_1 + c_2}{2})\mathbb{P}(U_n = k|\mathcal{R})N_{pd}(n).$$

Since h is a continuous function (defined on bounded and closed domain) there exists a real number $k^* \equiv k^*(PD)$ over the possible range of $3'$-ending telomere chains of cells accounted in $M(PD)$ such that

$$h(k^*)\frac{46}{2^{PD}} \sum_{pd \le PD} \sum_n \sum_k \mathbb{P}(V = k - \frac{c_1 + c_2}{2})\mathbb{P}(U_n = k|\mathcal{R})N_{pd}(n) =$$
$$= \frac{46}{2^{PD}} \sum_{pd \le PD} \sum_n \sum_k h(k)\mathbb{P}(V = k - \frac{c_1 + c_2}{2})\mathbb{P}(U_n = k|\mathcal{R})N_{pd}(n)$$

by the mean value theorem. If $\overline{k}_{PD}$ is a length mean of $3'$-ending telomere chains of cells accounted in $M(PD)$ we can estimate k^* with $\overline{k}_{PD}$. Hence

$$\frac{46}{2^{PD}} \sum_{pd \le PD} \sum_n \sum_k h(k)\mathbb{P}(V = k - \frac{c_1 + c_2}{2})\mathbb{P}(U_n = k|\mathcal{R})N_{pd}(n) \approx$$
$$\approx h(\overline{k}_{PD})\frac{46}{2^{PD}} \sum_{pd \le PD} \sum_n \sum_k \mathbb{P}(V = k - \frac{c_1 + c_2}{2})\mathbb{P}(U_n = k|\mathcal{R})N_{pd}(n).$$

Similarly by assuming that $k \mapsto \mathbb{P}(V = k - \frac{c_1+c_2}{2})$ is a continuous function we get the following approximation for each $pd \le PD$

$$\sum_n \sum_k \mathbb{P}(V = k - \frac{c_1 + c_2}{2})\mathbb{P}(U_n = k|\mathcal{R})N_{pd}(n) \approx \mathbb{P}(V = \overline{k}_{pd} - \frac{c_1 + c_2}{2})M(pd).$$

Hence

$$\mathrm{CP}(PD) \approx h(\overline{k}_{PD})\frac{46}{2^{PD}} \sum_{pd \le PD} \mathbb{P}(V = \overline{k}_{pd} - \frac{c_1 + c_2}{2})M(pd).$$

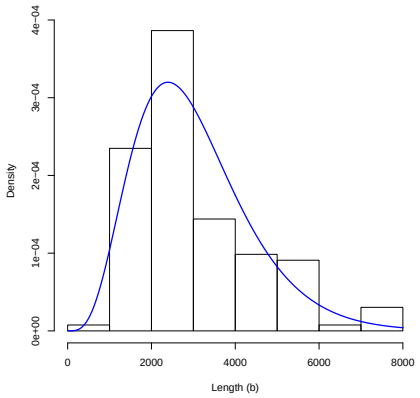

Figure A.8: The optimal fit of negative binomial distribution on data of extrachromosomal circle lengths measured from micrographs at PDs 32,42 and 52 (data taken from [18] with permission), with *standard deviation*=1369.72 and *mean*=3015.23.

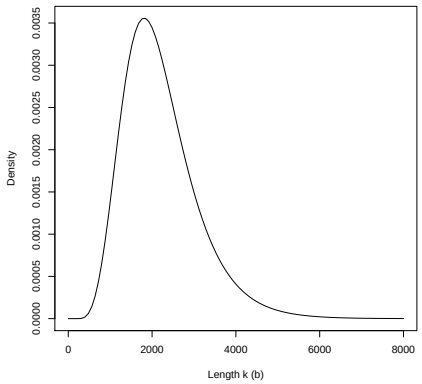

Figure A.9: Probability of abrupt shortening of a chromosome given the length of telomere sequence on the $3'$ end of chromosomal strand, i.e. $\mathbb{P}(\mathcal{A}|U_n = k) = \frac{a}{1+\left(\frac{k}{b}\right)^c}\mathbb{P}(V = k - \frac{c_1+c_2}{2})$ with $a = 24.470$, $b = 2016.97$ b, $c = 3.4802$.

Now we use data $\mathrm{CP}(PD)$ for $PD = 39, 49, 59$ from [9] to estimate the parameters of function h. In the first iteration we assume that $h \equiv h_0$ is a constant and we simulated data (by the algorithm from Section 2.2) to obtain numbers $M_0(pd) := M(pd)$, $\overline{k}_{pd,0} := \overline{k}_{pd}$ for $pd \leq PD$, $PD \in \{39, 49, 59\}$. From this numbers we calculated the correction factor

$$\omega_0(PD) := \frac{46}{2^{PD}} \sum_{pd \leq PD} \mathbb{P}(V = \overline{k}_{pd,0} - \frac{c_1 + c_2}{2}) M_0(pd).$$

Then we use LS-estimation procedure to estimate the first approximation $\hat{a}_1$, $\hat{b}_1$ and $\hat{c}_1$ of parameters a, b and c of function h:

$$(\hat{a}_1, \hat{b}_1, \hat{c}_1) = \mathrm{Argmin}_{a,b,c} \sum_{PD \in \{39,49,59\}} \left(\mathrm{CP}(PD) - h(\overline{k}_{PD,0}; a, b, c)\, \omega_0(PD)\right)^2. \tag{A.4}$$

Then, in the next iteration, we use these estimated parameters of h to simulate data $M_1(pd)$, $\overline{k}_{pd,1}$ for $pd \leq PD$, $PD \in \{39, 49, 59\}$, and estimate the next approximation of the parameters of h by the same LS procedure. We continue

this iterative procedure until the sum of squares in A.4 becomes at least of order 10^{-5}. Figure A.9 shows modelled probability $\mathbb{P}(\mathcal{A}|U_n = k)$ with the final estimates of parameters $\hat{a} = 24.470$, $\hat{b} = 2016.97$ b, $\hat{c} = 3.4802$. For LS-estimation, in order to minimize the sum of squares in A.4, we used R function *optim()*. Estimated parameters were numerically calculated by the conjugate gradients method (specified in the *optim()* function).

References

[1] L. Hayflick, P. S. Moorehead, The serial cultivation of human diploid cell strains, Experimental Cell Research 25 (1961) 585–621. doi:10.1016/0014-4827(61)90192-6.

[2] L. Hayflick, The limited in vitro lifetime of human diploid cell strains, Experimental Cell Research 37 (1965) 614–636.

[3] J. R. Smith, L. Hayflick, Variation in the life-span of clones derived from human diploid cell strains, Journal of Cell Biology 62 (1974) 48–53. doi:10.1083/jcb.62.1.48.

[4] J. R. Smith, R. G. Whitney, Intraclonal variation in proliferative potential of human diploid fibroblasts: stochastic mechanism for cellular aging, Science 207 (1980) 82–84. doi:10.1126/science.7350644.

[5] A. M. Olovnikov, A theory of marginotomy. the incomplete copying of template margin in enzymic - synthesis of polynucleotides and biological significance of the phenomenon, Journal of Theoretical Biology 41 (1973) 181—-190. doi:10.1016/0022-5193(73)90198-7.

[6] C. B. Harley, A. B. Futcher, C. Greider, Telomeres shorten during ageing of human fibroblasts, Nature 345 (1990) 458–460. doi:10.1038/345458a0.

[7] E. H. Blackburn, Telomere states and cell fates, Nature 408 (2000) 53–56. doi:10.1038/35040500.

[8] T. von Zglinicki, Oxidative stress shortens telomeres, Trends in Biochemical Sciences 27 (7) (2002) 339–344. doi:10.1016/S0968-0004(02)02110-2.

[9] I. Rubelj, Z. Vondraček, Stochastic mechanism of cellular aging - abrupt telomere shortening as a model for stochastic nature of cellular aging, Journal of Theoretical Biology 197 (4) (1999) 425–438. doi:10.1006/jtbi.1998.0886.

[10] D. A. Sinclair, L. Guarente, Extrachromosomal rdna circles - a cause of aging in yeast, Cell 91 (7) (1997) 1033–1042. doi:10.1016/S0092-8674(00)80493-6.

[11] C.-Y. Lin, H.-H. Chang, K.-J. Wu, S.-F. Tseng, C.-C. Lin, C.-P. Lin, S.-C. Teng, Extrachromosomal telomeric circles contribute to rad52-, rad50-, and polymerase δ-mediated telomere-telomere recombination in saccharomyces cerevisiae, Eukaryotic Cell 4 (2) (2005) 327–336. doi:10.1128/EC.4.2.327-336.2005.

[12] S. Cohen, A. Regev, S. Lavi, Small polydispersed circular dna (spcdna) in human cells: association with genomic instability, Oncogene 14 (8) (1997) 977–985. doi:10.1038/sj.onc.1200917.

[13] B. Li, S. P. Jog, S. Reddy, L. Comai, Wrn controls formation of extrachromosomal telomeric circles and is required for trf2δb - mediated telomere shortening, Molecular and Cellular Biology 28 (2008) 1892–1904. doi:10.1128/MCB.01364-07.

[14] S. A. Compton, J. H. Choi, A. J. Cesare, S. Ozgur, J. D. Griffith, Xrcc3 and nbs1 are required for the production of extrachromosomal telomeric circles in human alternative lengthening of telomere cells, Cancer Research 67 (2007) 1513–1519. doi:10.1158/0008-5472.CAN-06-3672.

[15] R. C. Wang, A. Smogorzewska, T. de Lange, Homologous recombination generates t-loop-sized deletions at human telomeres, Cell 119 (2004) 355–368. doi:10.1016/j.cell.2004.10.011.

[16] Y. Wang, G. Ghosh, E. A. Hendrickson, Ku86 represes lethal telomere deletion event in human somatic cells, Proceedings of the National Academy of Sciences of the United States of America 106 (30) (2009) 12430–12435. doi:10.1073/pnas.0903362106.

[17] A. J. Cesare, J. D. Griffith, Telomeric dna in alt cels is characterized by free telomeric circles and heterogeneous t-loops, Molecular and Cellular Biology 24 (2004) 9948–9957. doi:10.1128/MCB.24.22.9948-9957.2004.

[18] N. . Vidaček, A. Ćukušić, M. Ivanković, H. Fulgosi, M. Huzak, J. R. Smith, I. Rubelj, Abrupt telomere shortening in normal human fibroblasts, Experimental Gerontology 45 (3) (2010) 235–242. doi:10.1016/j.exger.2010.01.009.

[19] K. Sakabe, R. Okazaki, A unique property of the replicating region of chromosomal dna, Biochimica et Biophysica Acta 129 (3) (1966) 651–654. doi:10.1016/0005-2787(66)90088-8.

[20] A. M. Olovnikov, Principle of marginotomy in template synthesis of polynucleotides, Dokl Akad Nauk SSSR 201 (6) (1971) 1496—-1499. doi:10.3410/f.717968476.15528075.

[21] S. Eugene, T. Bourgeron, Z. Xu, Effects of initial telomere length distribution on senescence onset and heterogeneity, Journal of Theoretical Biology 413 (2017) 58–65. doi:10.1016/j.jtbi.2016.11.010.

[22] N. Arkus, A mathematical model of cellular apoptosis and senescence through the dynamics of telomere loss, Journal of Theoretical Biology 235 (1) (2005) 13–32. doi:10.1016/j.jtbi.2004.12.016.

[23] K. E. Huffman, S. D. Levene, V. M. Tesmer, S. J. W., W. E. Wright, Telomere shortening is proportional to the size of the g-rich telomeric 3'-overhang, The Journal of Biological Chemistry 275 (26) (2000) 19719–19722. doi:10.1074/jbc.M002843200.

[24] D. M. Baird, Telomere dynamics in human cells, Biochimie 90 (1) (2008) 116–121. doi:10.1016/j.biochi.2007.08.003.

[25] O. Arino, M. Kimmel, G. F. Webb, Mathematical modelling of the loss of telomere sequences, Journal of Theoretical Biology 177 (1) (1995) 45–57. doi:10.1006/jtbi.1995.0223.

[26] M. Z. Levy, R. C. Allsopp, A. B. Futcher, C. W. Greider, C. B. Harley, Telomere end-replication problem and cell aging, Journal of Molecular Biology 225 (4) (1992) 951–960. doi:10.1016/0022-2836(92)90096-3.

[27] P. Olofsson, M. Kimmel, Stochastic models of telomere shortening, Mathematical Biosciences 158 (1) (1999) 75–92.

[28] E. S. Epel, E. H. Blackburn, J. Lin, F. S. Dhabar, N. E. Adler, J. D. Morrow, R. M. Cawthon, Accelerated telomere shortening in response to life stress, Proceedings of the National Academy of Sciences 101 (2004) 17312–17315. doi:10.1073/pnas.0407162101.

[29] T. von Zglinicki, R. Pilger, N. Sitte, Accumulation of single-strand breaks is the major cause of telomere shortening in human fibroblasts, Free Radical Biology & Medicine 28 (1) (2000) 64–74.

[30] P. Olofsson, A branching proces model of telomere shortening, Communications in Statistics - Stochastic Models 16 (1) (2000) 167–177. doi:10.1080/15326340008807581.

[31] Q. Qi, Mathematical modelling of telomere dynamics, Ph.D. thesis, The University of Nottingham, available at http://etheses.nottingham.ac.uk (2011).

[32] R. D. Portugal, M. G. Land, B. F. Svaiter, A computational model for telomere-dependent cell-replicative aging, Biosystems 91 (1) (2008) 262–267. doi:10.1016/j.biosystems.2007.10.003.

[33] T. Bourgeron, Z. Xu, M. Doumic, M. T. Teixeira, The asymmetry of telomere replication contributes to replicative senescence heterogeneity, Scientific Reports 5, article number: 15326. doi:10.1038/srep15326.

[34] I. A. Rodriguez-Brenes, C. S. Peskin, Quantitative theory of telomere length regulation and cellular senescence, Proceedings of the National Academy of Sciences 107 (12) (2010) 5387–5392. doi:10.1073/pnas.0914502107.

[35] P. Olofsson, A. Bertuch, Modeling growth and telomere dynamics in saccharomyces cerevisiae, Journal of Theoretical Biology 263 (3) (2010) 353–359. doi:10.1016/j.jtbi.2009.12.004.

[36] J. Grasman, H. M. Salomons, S. Verhulst, Stochastic modeling of length-dependent telomere shortening in corvus monedula, Journal of Theoretical Biology 282 (1) (2011) 1–7. doi:10.1016/j.jtbi.2011.04.026.

[37] B. Britt-Compton, J. Rowson, M. Locke, I. Mackenzie, D. Kipling, D. M. Baird, Structural stability and chromosome-specific telomere length is governed by cis-acting determinants in humans, Human Molecular Genetics 15 (5) (2006) 725–733. doi:10.1093/hmg/ddi486.

[38] Z. Xu, K. D. Duc, D. Holcman, M. T. Teixeira, The length of the shortest telomere as the major determinant of the onset of replicative senescence, Genetics 194 (4) (2013) 847–857. doi:10.1534/genetics.113.152322.

[39] S. Lambert, B. Froget, A. Carr, Arrested replication fork processing: interplay between checkpoints and recombination., DNA Repair (Amst) 6 (7) (2007) 1042–1061. doi:10.1016/j.dnarep.2007.02.024.

[40] U. M. Martens, E. A. Chavez, S. S. Poon, C. Schmoor, P. M. Lansdorp, Accumulation of short telomeres in human fibroblasts prior to replicative senescence, Experimental Cell Research 256 (2000) 291–299. doi:10.1006/excr.2000.4823.

[41] J. op den Buijs, P. P. van den Bosch, M. W. Musters, N. A. van Riel, Mathematical modeling confirms the length-dependency of telomere shortening, Mechanisms of Ageing and Development 125 (6) (2004) 437–444. doi:10.1016/j.mad.2004.03.007.

[42] P. M. Lansdorp, N. Verwoerd, F. van de Rijke, V. Dragowska, M. Little, R. Dirks, A. Raap, H. Tanke, Heterogeneity in telomere length of human chromosomes, Human Molecular Genetics 5 (1996) 685–691. doi:10.1093/hmg/5.5.685.

[43] A. Ćukušić Kalajzić, N. Škrobot Vidaček, M. Huzak, M. Ivanković, I. Rubelj, Telomere q-pna-fish - reliable results from stochastic signals, PLoS ONE 9 (3), e92559. doi:10.1371/journal.pone.0092559.
URL http://journals.plos.org/plosone/article?id=10.1371/journal.pone.0092559